Flexible Crystalline Silicon Nanomembrane Photonic Crystal Microcavity

Xiaochuan Xu[1,2,*], Harish Subbaraman[2,*], Amir Hosseini[2], Swapnajit Chakravarty[2], and Ray T. Chen[1]
[1]The University of Texas at Austin – 10100 Burnet Rd, PRC/MER 160, Austin, TX 78758 (USA)
[2]Omega Optics, Inc – 10306 Sausalito Dr, Austin, TX 78731 (USA)
**authors contribute equally*
Author e-mail address: (xiaochuan.xu@utexas.edu, raychen@uts.cc.utexas.edu)

Abstract: We for the first time demonstrated a flexible crystalline silicon nanomembrane photonic crystal microcavity, which shows a quality factor of 22000 and could be bent to a radius of 5 mm.
OCIS codes: (350.4238) Nanophotonics and photonic crystals; (310.6628) Subwavelength Structures, Nanostructuresl

Nanomembrane research has attracted a lot of attention over the last decade, due to the ability to develop light-weight and conformal devices.[1] Flexible and conformal electronic devices promise tremendous applications in the areas of wearable and biomedical electronics, which are unthinkable using conventional material systems. Benefits on a similar scale are also foreseeable for photonic components. However, the difficulty in transferring intricate photonic devices, has deterred widespread developmental activities. The performance of photonic devices heavily relies on the integrity of the geometry, and the tolerance is astonishingly low. The "peel" and "stamp" operations, which are essentials of the conventional stamp printing process, are unfortunately the source of geometrical imperfections. In this paper, we introduce a high yield transfer method and demonstrate transferring L13 photonic crystal microcavity onto Kapton film.

Figure 1 a-d briefly depict the transfer sequence. The first step (Fig.1a) involves electron beam lithography (EBL) and reactive ion etch (RIE) to define silicon photonic devices on a silicon-on-insulator (SOI) chip with 250 nm single crystal silicon layer, 3 μm buried oxide layer (BOX), and 675 μm silicon handle. The patterned chip is flipped over and bonded onto the Kapton substrate through adhesive bonding (Fig.1b). The native oxide on SOI is removed by 1:6 buffered oxide etchant (BOE) in advance to improve the adhesion. The Kapton film is mounted on a rigid substrate. SU-8 is spun coated on the Kapton film and the chip, both of which are baked at 65 ^{o}C for an extended period of time to improve the surface quality, because SU-8 has impressive self-planarization capability when heated up to a temperature above its glass transition temperature. [2] The SU-8 layer on the Kapton film is partially cured to generate Lewis acid, which can initiate the crosslink when the unexposed SU-8 on SOI is brought in contact. After bonding, the silicon handle is removed by mechanic polishing, followed by deep reactive ion etching (DRIE),

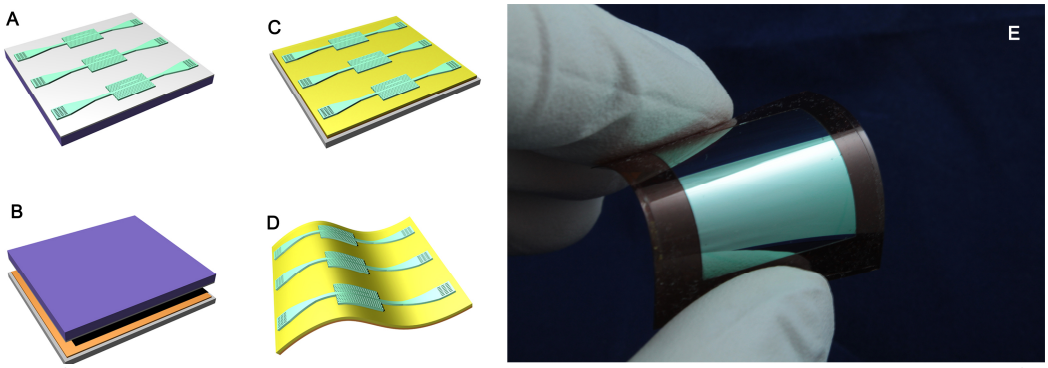

Fig. 1. (a~d)Transfer process. (a) Pattern the photonic crystal microcavity on SOI. (b) Flip bond the SOI chip on to the Kapton film with SU-8 epoxy. (c) Remove the handle and BOX layer with mechanic polishing, DRIE, and wet etching. (d) Peel off the Kapton film from the mechanic support. (e) The optical image of transferred sample.

as shown in Fig.1c. The DRIE process is tailored to control the thermal budget. The etch rate is about 2.7 μm /cycle with a selectivity around 80 to silicon dioxide, making the 3 μm thick BOX a good etching stopping layer, which is removed by concentrated hydrofluoric acid (HF) afterwards. Finally, Kapton is peeled up from the rigid carrier (Fig.1d). Fig. 1e shows the transferred 2 cm× 2 cm silicon nanomembrane. The advantages of adhesive bonding include the relatively low bonding temperatures, the insensitivity to the topology of the bonding surfaces, the compatibility with standard complementary metal-oxide semiconductor (CMOS) process, and the ability to join

practically any materials. During the transfer procedure, the whole photonic devices are embedded in the SU-8 layer, which provide mechanic protections and thus preventing the devices from mechanic failures.

Figure 2a illustrates the schematic of the L13 photonic crystal microcavity comprised of a linear photonic crystal microcavity coupled with a classical W1 photonic crystal waveguide (PCW). The lattice constant *a* is 392.5 nm and the hole radius *r* is 108 nm. The thickness of the slab *t* is 250 nm. W1 waveguide is formed by removing one row of holes along Γ–K direction. An eight-period photonic crystal adiabatic taper is designed to improve the coupling efficiency between strip and photonic crystal waveguides. The dispersion relation of the W1 waveguide, simulated by three dimensional plane wave expansion (PWE), is shown in Fig.2b. The cavity is located two rows away from the W1 waveguide. The two holes at the ends of the cavity are moved outwards by s=0.15a to increase quality factor (Q).[3] Subwavelength grating couplers are used for in and output coupling.[4] Fig. 2c shows the transmission spectra after transfer with water top cladding (blue) and glycerol top cladding (red), which have a Q of 9000 and

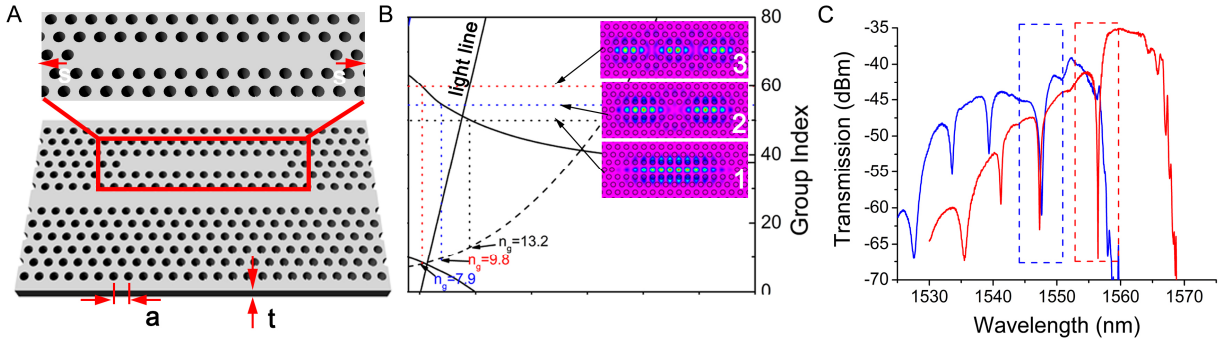

Fig. 2. (a)Schematic of the L13 Cavity. (b) Band diagram of the photonic crystal waveguide and the L13 cavity. Inset: the mode distribution of the three resonance modes. (c)The transmission spectra after transfer with water top cladding (blue) and with glycerol top cladding (red).

22000, respectively. The device can also be used as a refractive index sensor with a sensitivity of 68 nm/RIU.

The bending characteristic of the flexible microcavity is investigated with the measurement set up described in Fig. 3a. The two ends of the film are constrained on the jaws of a caliper, but allowed to rotate freely. The film can be buckled up by sliding the movable jaw inwards. The bending deforms the lattice structure and therefore distorts the symmetry in reciprocal lattice (the insets of Fig. 3b and c). The bending induced strain will also cause index variation. The combination of the two effects causes the wavelength shift. The red dots in Fig. 3b and c are the experimental results showing the correlation between strain and resonant wavelength for longitudinal face-out (LFO) bending and longitudinal face-in bending (LFI). The sensitivity are 0.673 pm/με and 0.656 pm/με, respectively. The 2D simulation with finite element method (FEM) and finite difference time domain (FDTD) shows a good match with the experimental results. The quality factor stays constant for different bending radius as shown by the circles in Fig. 3b and c.

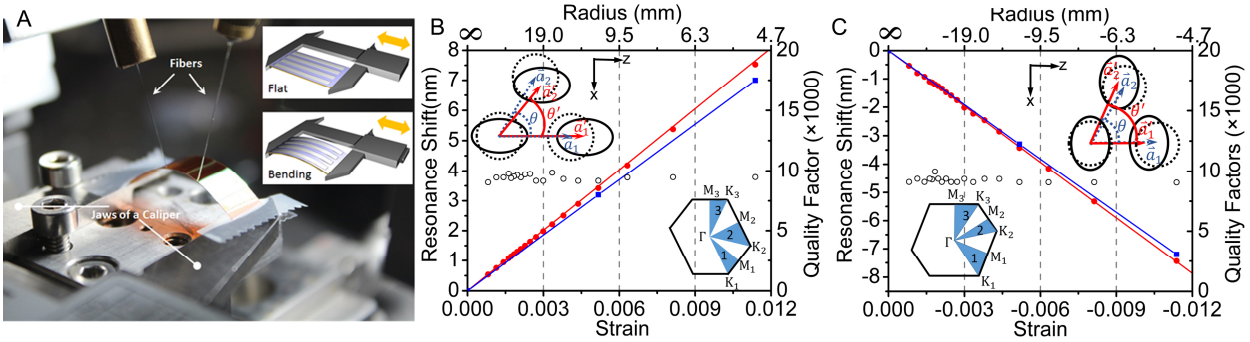

Fig. 3. (a) Bending testing set up. The experimental (red) and simulation (blue) results of (b) LFO and (c) LFI. The circles are the quality factor

In conclusion, we demonstrated a flexible single crystal silicon nanomembrane photonic crystal microcavity which shows amazing flexibility and high quality factor.

References

1. Kim, D. H. et al. Epidermal Electronics. Science 333, 838-843 (2011)
2. S. Keller, et al. "Processing of thin SU-8 films," Journal of Micromechanics and Microengineering **18**(2008).
3. Y. Akahane, et al, "High-Q photonic nanocavity in a two-dimensional photonic crystal," Nature **425**, 944-947 (2003).
4. Xu, X. et al. Complementary metal–oxide–semiconductor compatible high efficiency subwavelengthgrating couplers for silicon integrated photonics, Appl. Phys. Lett. 101, 031109 (2012)

Flexible Crystalline Silicon Nanomembrane Photonic Crystal Microcavity

Xiaochuan Xu[1,2,*], Harish Subbaraman[2,*], Amir Hosseini[2], Swapnajit Chakravarty[2], and Ray T. Chen[1]
[1]The University of Texas at Austin – 10100 Burnet Rd, PRC/MER 160, Austin, TX 78758 (USA)
[2]Omega Optics, Inc – 10306 Sausalito Dr, Austin, TX 78731 (USA)
**authors contribute equally*
Author e-mail address: (xiaochuan.xu@utexas.edu, raychen@uts.cc.utexas.edu)

Abstract: We for the first time demonstrated a flexible crystalline silicon nanomembrane photonic crystal microcavity, which shows a quality factor of 22000 and could be bent to a radius of 5 mm.
OCIS codes: (350.4238) Nanophotonics and photonic crystals; (310.6628) Subwavelength Structures, Nanostructuresl

Nanomembrane research has attracted a lot of attention over the last decade, due to the ability to develop light-weight and conformal devices.[1] Flexible and conformal electronic devices promise tremendous applications in the areas of wearable and biomedical electronics, which are unthinkable using conventional material systems. Benefits on a similar scale are also foreseeable for photonic components. However, the difficulty in transferring intricate photonic devices, has deterred widespread developmental activities. The performance of photonic devices heavily relies on the integrity of the geometry, and the tolerance is astonishingly low. The "peel" and "stamp" operations, which are essentials of the conventional stamp printing process, are unfortunately the source of geometrical imperfections. In this paper, we introduce a high yield transfer method and demonstrate transferring L13 photonic crystal microcavity onto Kapton film.

Figure 1 a-d briefly depict the transfer sequence. The first step (Fig.1a) involves electron beam lithography (EBL) and reactive ion etch (RIE) to define silicon photonic devices on a silicon-on-insulator (SOI) chip with 250 nm single crystal silicon layer, 3 μm buried oxide layer (BOX), and 675 μm silicon handle. The patterned chip is flipped over and bonded onto the Kapton substrate through adhesive bonding (Fig.1b). The native oxide on SOI is removed by 1:6 buffered oxide etchant (BOE) in advance to improve the adhesion. The Kapton film is mounted on a rigid substrate. SU-8 is spun coated on the Kapton film and the chip, both of which are baked at 65 ^{o}C for an extended period of time to improve the surface quality, because SU-8 has impressive self-planarization capability when heated up to a temperature above its glass transition temperature. [2] The SU-8 layer on the Kapton film is partially cured to generate Lewis acid, which can initiate the crosslink when the unexposed SU-8 on SOI is brought in contact. After bonding, the silicon handle is removed by mechanic polishing, followed by deep reactive ion etching (DRIE),

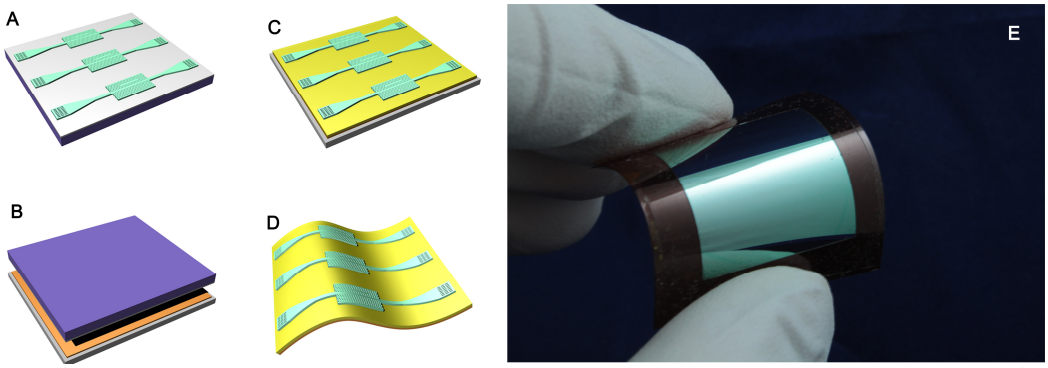

Fig. 1. (a~d)Transfer process. (a) Pattern the photonic crystal microcavity on SOI. (b) Flip bond the SOI chip on to the Kapton film with SU-8 epoxy. (c) Remove the handle and BOX layer with mechanic polishing, DRIE, and wet etching. (d) Peel off the Kapton film from the mechanic support. (e) The optical image of transferred sample.

as shown in Fig.1c. The DRIE process is tailored to control the thermal budget. The etch rate is about 2.7 μm /cycle with a selectivity around 80 to silicon dioxide, making the 3 μm thick BOX a good etching stopping layer, which is removed by concentrated hydrofluoric acid (HF) afterwards. Finally, Kapton is peeled up from the rigid carrier (Fig.1d). Fig. 1e shows the transferred 2 cm× 2 cm silicon nanomembrane. The advantages of adhesive bonding include the relatively low bonding temperatures, the insensitivity to the topology of the bonding surfaces, the compatibility with standard complementary metal-oxide semiconductor (CMOS) process, and the ability to join

practically any materials. During the transfer procedure, the whole photonic devices are embedded in the SU-8 layer, which provide mechanic protections and thus preventing the devices from mechanic failures.

Figure 2a illustrates the schematic of the L13 photonic crystal microcavity comprised of a linear photonic crystal microcavity coupled with a classical W1 photonic crystal waveguide (PCW). The lattice constant *a* is 392.5 nm and the hole radius *r* is 108 nm. The thickness of the slab *t* is 250 nm. W1 waveguide is formed by removing one row of holes along Γ–K direction. An eight-period photonic crystal adiabatic taper is designed to improve the coupling efficiency between strip and photonic crystal waveguides. The dispersion relation of the W1 waveguide, simulated by three dimensional plane wave expansion (PWE), is shown in Fig.2b. The cavity is located two rows away from the W1 waveguide. The two holes at the ends of the cavity are moved outwards by s=0.15a to increase quality factor (Q).[3] Subwavelength grating couplers are used for in and output coupling.[4] Fig. 2c shows the transmission spectra after transfer with water top cladding (blue) and glycerol top cladding (red), which have a Q of 9000 and

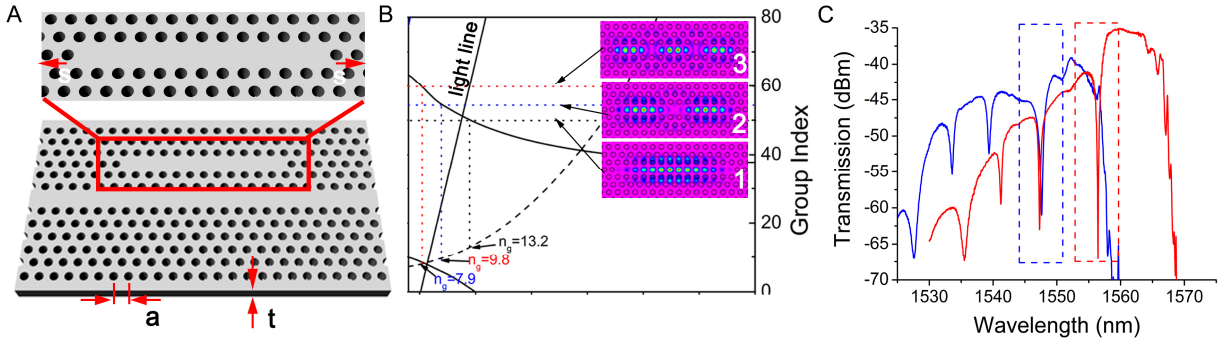

Fig. 2. (a)Schematic of the L13 Cavity. (b) Band diagram of the photonic crystal waveguide and the L13 cavity. Inset: the mode distribution of the three resonance modes. (c)The transmission spectra after transfer with water top cladding (blue) and with glycerol top cladding (red).

22000, respectively. The device can also be used as a refractive index sensor with a sensitivity of 68 nm/RIU.

The bending characteristic of the flexible microcavity is investigated with the measurement set up described in Fig. 3a. The two ends of the film are constrained on the jaws of a caliper, but allowed to rotate freely. The film can be buckled up by sliding the movable jaw inwards. The bending deforms the lattice structure and therefore distorts the symmetry in reciprocal lattice (the insets of Fig. 3b and c). The bending induced strain will also cause index variation. The combination of the two effects causes the wavelength shift. The red dots in Fig. 3b and c are the experimental results showing the correlation between strain and resonant wavelength for longitudinal face-out (LFO) bending and longitudinal face-in bending (LFI). The sensitivity are 0.673 pm/με and 0.656 pm/με, respectively. The 2D simulation with finite element method (FEM) and finite difference time domain (FDTD) shows a good match with the experimental results. The quality factor stays constant for different bending radius as shown by the circles in Fig. 3b and c.

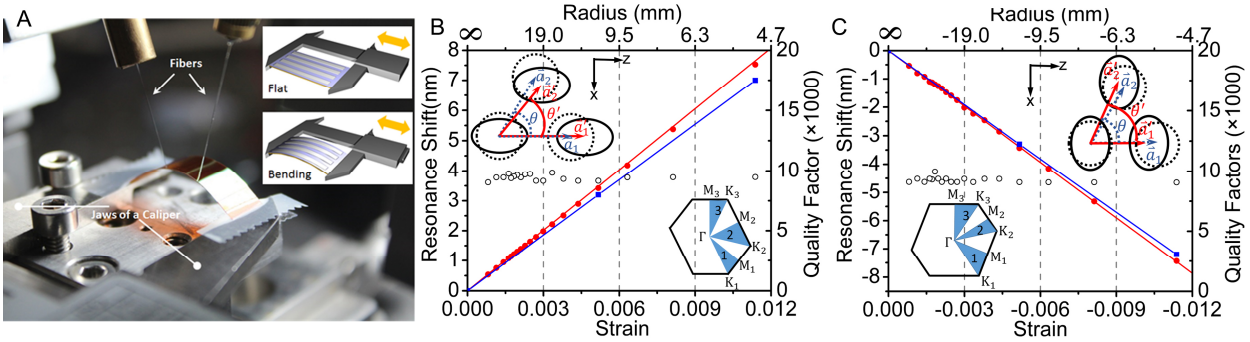

Fig. 3. (a) Bending testing set up. The experimental (red) and simulation (blue) results of (b) LFO and (c) LFI. The circles are the quality factor

In conclusion, we demonstrated a flexible single crystal silicon nanomembrane photonic crystal microcavity which shows amazing flexibility and high quality factor.

References

1. Kim, D. H. et al. Epidermal Electronics. Science 333, 838-843 (2011)
2. S. Keller, et al. "Processing of thin SU-8 films," Journal of Micromechanics and Microengineering **18**(2008).
3. Y. Akahane, et al, "High-Q photonic nanocavity in a two-dimensional photonic crystal," Nature **425**, 944-947 (2003).
4. Xu, X. et al. Complementary metal–oxide–semiconductor compatible high efficiency subwavelengthgrating couplers for silicon integrated photonics, Appl. Phys. Lett. 101, 031109 (2012)